Composites Part B 198 (2020) 108229

Contents lists available at ScienceDirect

Composites Part B

journal homepage: www.elsevier.com/locate/compositesb

# Enhancing indentation and impact resistance in auxetic composite materials

Tiantian Li [a], Fan Liu [b], Lifeng Wang [b,*]

[a] Department of Engineering, University of Cambridge, Cambridge, CB2 1PZ, United Kingdom
[b] Department of Mechanical Engineering, Stony Brook University, Stony Brook, New York, 11794, USA

ARTICLE INFO

*Keywords:*
Auxetics
3D printing
Indentation stiffness
Composites
Lattice materials

ABSTRACT

Auxetic materials exhibiting a negative Poisson's ratio are of great research interest due to their unusual mechanical responses and a wide range of potential deployment. However, due to the cellular structure and the bending or rotation deformation nature of the elements in auxetic materials, they usually have relative low stiffness, limiting their applications where high stiffness, strength, hardness, and energy absorption are simultaneously desired. To overcome this limitation, we apply the auxetic lattice structures as the reinforcements combining with the nearly incompressible soft materials as the matrix to create a class of high-performance composites. This coupled geometry and material design concept is enabled by the state-of-the-art additive manufacturing technique. Guided by static and dynamic experimental testing, we systematically study the indentation behavior of the 3D printed auxetics reinforced composites and achieve a significant enhancement of their indentation stiffness and impact resistance compared with the non-auxetic reinforced composites. By digital image correlation processing of experimental tests and numerical simulation, this improved mechanical performance is found due to two deformation mechanisms. The first mechanism is the negative Poisson's ratio effect of the auxetic reinforcements, which makes the matrix in a state of biaxial compression during indentation and impact and hence provides additional support. The second mechanism is the negative Poisson's ratio effect of the overall composites, which makes the auxetic reinforced composites denser at the site of the indentation and therefore are more resistant to indentation. The results show that auxetic structures can lead to design stiffer, harder and tougher composite materials. The material design strategy provides insights into the development of classes of novel auxetic composites with a wide range of mechanical and structural applications.

## 1. Introduction

Auxetic materials are a new type of mechanical metamaterials which contracts/expands transversally when they are axially compressed/stretched. Owning to their unusual mechanical behavior, auxetic materials have increasing application potentials in medical devices for foldable stents [1], energy absorption systems for protect from impacts [2–4], electronic systems for smart sensors [5,6], and textile industry [7]. Since the 1980s, auxetic behavior has been reported in many natural materials, including cubic metals [8], zeolites [9], natural layered ceramics [10], silicon dioxides [11], single-layer graphene [12] and 2D protein crystals [13]. Meanwhile, after the first development of 3D polymeric foams with isotropic auxetic behavior by Lakes [14], man-made auxetic materials and structures has been fabricated and synthesized from the macroscopic down to molecular levels. Among them, there are planar foams [15], honeycomb [16], chiral lattices [17], wavy lattices [18,19], rigid rotating hexamers or squares [20], origami/kirigami based metamaterials [21] and hierarchical metamaterials with fractal cuts [22].

Comparing with conventional materials, auxetic materials and structures possess many superior properties such as shear resistance [23], fracture resistance [24], synclastic behavior [25], variable permeability [26] and energy absorption [4,27,28]. One significant improvement for auxetic materials is indentation resistance. When an object hits an auxetic material and compresses it in one direction, the auxetic material contracts laterally – material 'flows' into the vicinity of the impact. This creates an area of denser material, which is resistant to indentation [29]. According to the classical theory of elasticity, the indentation resistance is closely related to the material hardness ($H$), which could be correlated to the Poisson's ratio by:

* Corresponding author.
*E-mail address:* lifeng.wang@stonybrook.edu (L. Wang).

https://doi.org/10.1016/j.compositesb.2020.108229
Received 4 February 2020; Received in revised form 29 May 2020; Accepted 14 June 2020
Available online 2 July 2020

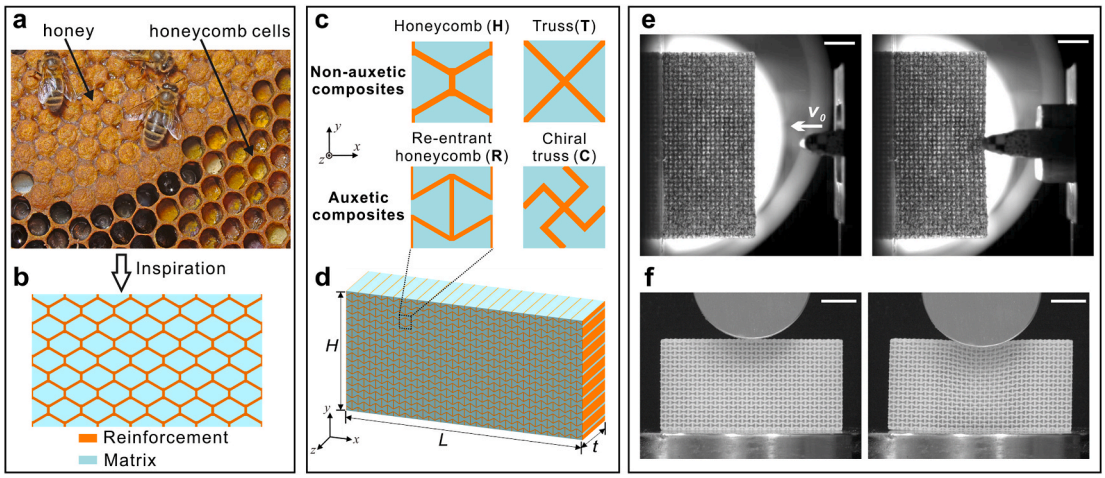


**Fig. 1.** (a) Natural honeycombs have a composite structure with comb cells and stored honey and pollen. (b) Bio-inspired composite structures with stiff lattice reinforcement and soft matrix. (c) Unit cell of lattice reinforced composites with non-auxetic lattice (regular honeycomb and regular truss) and auxetic lattice (re-entrant honeycomb and chiral truss). (d) The specimen for indentation and impact tests. (e) Schematics of the impact test show the specimen before impact and at impact. (f) Schematics of the indentation test show the specimens before indentation and at finite indentation. Scale bar: 1 cm.

$$H \propto \left[\frac{E}{(1-\nu^2)}\right]^n, \tag{1}$$

where $E$ is Young's modulus, $\nu$ is the Poisson's ratio of the base materials and $n$ is 1 for a cylinder indenter and 2/3 for a spherical indenter. For isotropic materials, $\nu$ can be presented as: $\nu = [3K/G - 2]/[2(3K/G + 1)]$, where $K$ is bulk modulus and $G$ is shear modulus. This formula defines numerical limits of Poisson's ratio for isotropic bulk materials as, $-1 \le \nu \le 0.5$ for $0 \le K/G \le \infty$. It can be clearly seen that, as $\nu$ approaches $-1$, the indentation resistance tends to infinity [30]. Starting from this point, the presence of a negative $\nu$ resulted in enhancement of the hardness has been first experimentally observed in ultra-high molecular weight polyethylene [31] and auxetic polyethylene foams [32]. However, after that, fewer real auxetic materials have been reported with improved indentation behavior comparing with conventional materials. This is because the modulus $E$ for auxetic material is usually lower than their non-auxetic counter-parts [33]. Auxetic materials are mostly cellular materials and their deformation mechanisms are bending or rotation dominated, which also limits their applications where lightweight, high stiffness, strength and energy absorption are simultaneously desired.

To overcome this limitation, recently we have applied the auxetic lattice structures as the reinforcements combining with the nearly incompressible soft materials as the matrix to create a class of high-performance composites. These multi-material auxetics or auxetic composites are enabled by the state-of-the-art additive manufacturing technique. From our previous studies [2], we have found that these 3D printed auxetic composites achieved a significant enhancement of their stiffness and energy absorption under uniaxial compression. However, an experimental observation of indentation behavior of these auxetic materials is still lacking and especially the mechanism accounting for the effect of negative Poisson's ratio on the indentation resistance is not well explained.

In this paper, we have fabricated four groups of composite materials consisting of glassy polymer as reinforcements and incompressible soft elastomer as the filled matrix. Two type auxetic lattices and their counter-part non-auxetic lattices as the reinforcement structures are designed. Static and dynamic indentation tests are conducted to investigate the indentation behavior of these composite materials. Finite element simulations are performed to provide additional insights to quantitatively understand the effects of Poisson's ratio and volume fraction of the reinforcements on the indentation behavior of these auxetic reinforced composites.

## 2. Materials and methods

### 2.1. Design of auxetic lattice reinforced composites

The model system of the lattice reinforced composites studied here is inspired from the natural honeycomb structures which combine the stiff lattice reinforcement and soft matrix. Natural honeycombs consist of comb cells and stored honey and pollen as shown in Fig. 1a–b. The comb cells are constructed from wax secreted by worker bees which have long been a paradigm for engineering cellular structures. However, the stored honey is an amorphous solid which is relative softer than the comb cells. The comb cells and stored honey formed a typical composite structure with a lattice structure and its inverse domains. Here, four types of lattice reinforced composites are designed: re-entrant honeycomb reinforced composites, chiral lattice reinforced composites, regular honeycomb reinforced composites and truss reinforced composites (Fig. 1c). For detailed geometrical parameters, we first fix the same square unit cell size for all designs. For honeycomb (labeled as **H**) and re-entrant honeycomb (labeled as **R**) lattices, we assign the angles between the straight struts and inclined struts as 120° and 60°. For chiral lattice (labeled as **C**) and truss lattice (labeled as **T**), we assign the angles of all the cross struts as 90°. From our previous compressive test results [2], the measured initial Poisson's ratios are 0.5 for honeycomb reinforced composite; −0.5 for re-entrant honeycomb reinforced composite, −0.3 for chiral lattice reinforced composite and 1 for truss reinforced composite. Finally, the symmetry and volume distribution in these structures can be precisely controlled by tailoring the thickness of ligaments in each lattice structure.

### 2.2. Sample fabrication

The prototypes of stiff lattice reinforcement/soft matrix composite materials are fabricated using a multi-material 3D-printer Objet Connex260. We use two photo-sensitive polymeric materials, an acrylic-based photopolymer, VeroWhite (VW), and a soft elastomeric material, TangoPlus (TP). The transparent soft matrix is printed in TP (Young's modulus ~0.77 MPa), and the stiffer lattice reinforcement is printed in VW (Young's modulus ~1.5 GPa). The specimens shown in Fig. 1d for indentation and impact tests consist of 20 × 10 unit cells, resulting in the total height of the specimens is $H = 30$ mm, the length is $L = 60$ mm. Focusing on the 2D in-plane mechanical behavior of these structures, the thickness of the specimens is 20 mm. The minimum geometric size of the lattice reinforcement in the composites is about

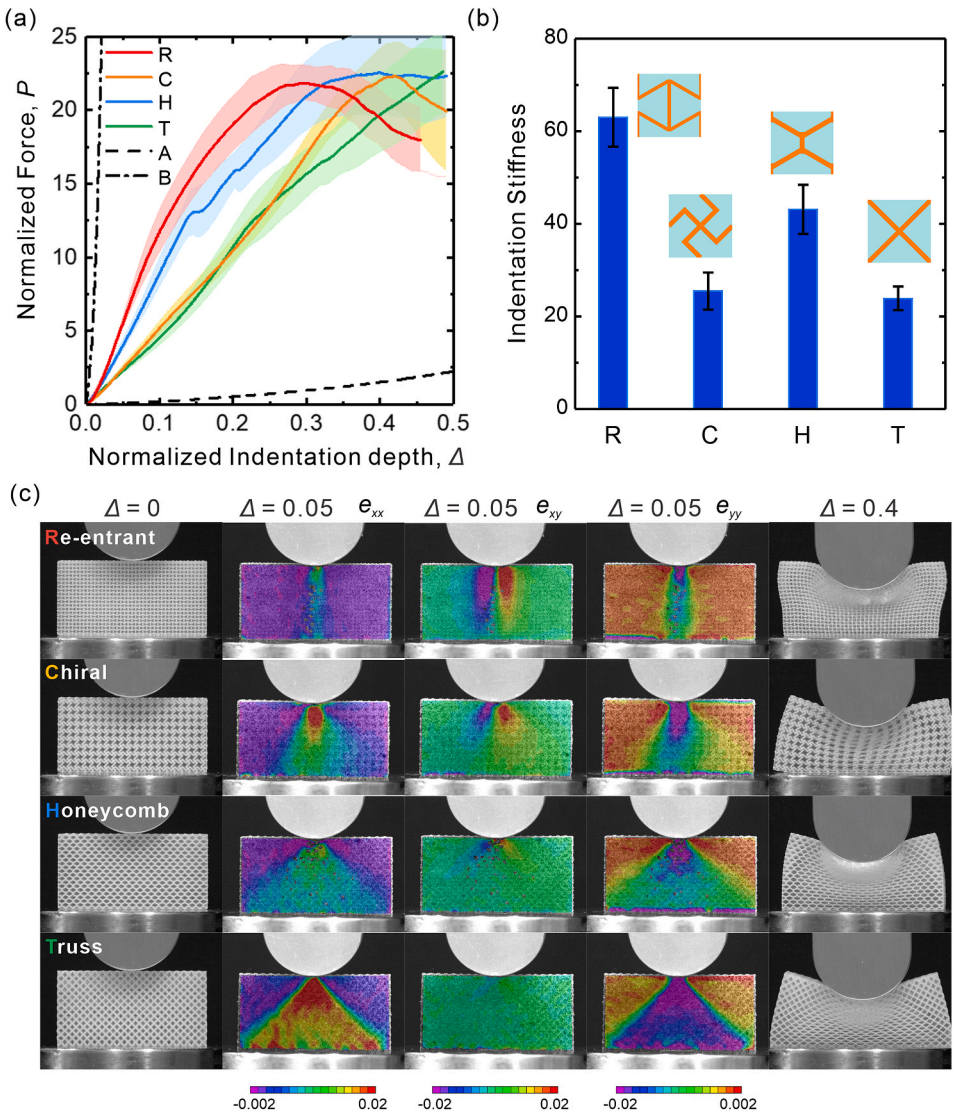


**Fig. 2.** Mechanical response of the 3D-printed lattice reinforced composites during indentation tests. (a) Force *vs.* indentation depth for four different composites with re-entrant honeycomb, chiral truss, regular honeycomb, regular truss designs and two homogeneous pure materials (VeroWhite and TangoPlus). (b) Relative indentation stiffness *vs.* composites with different lattice topology reinforcements. (c) The first column is for composites subjected to indentation depth $\Delta = 0.0$; experimental strain contours of composites using digital image correlation at indentation depth $\Delta = 0.05$ are in column (2), (3) and (4) as strain in the x-direction, shear strain and strain in the y-direction, respectively; the column (5) is for composites subjected to indentation depth $\Delta = 0.4$.

120 μm, which is one order of magnitude greater than the minimum resolution (16 μm) provided by the 3D printer. Considering the anisotropic nature of the 3D printing, all the specimens are printed along the same orientation to avoid the influence of the layer orientation on the mechanical properties of the material. The as-fabricated specimens are kept at room temperature for 7 days to allow for the saturation of the curing.

### 2.3. Mechanical testing

To capture the mechanical indentation behavior of the 3D printed lattice reinforced composites, indentation tests and dynamic impact tests are used (see Fig. 1e and f). The indentation tests are performed using an MTS mechanical tester (C43) and a cylindrical indenter with a radius of 20 mm. All the indentation tests are conducted in a quasi-static regime with an indenter velocity of 0.05 mm/s, corresponding to a nominal engineering strain rate of 0.00167/s. Dynamic tests are performed using a modified split Hopkinson pressure bar (SHPB) system [34]. Images of the specimens at various loading conditions are taken at a rate of 60000 FPS by a high-speed imaging camera (Photron SA1.1). Impact speed (3 m/s to 10 m/s) is achieved by controlling the pressure of the gas reservoir. When the control valve is opened, the high-pressure air accelerates the striker which then transfers its momentum to the impactor that impacts the specimen with the designed impact loading condition. The specimens for the impact tests are the same as the ones for the indentation tests. The mass of the impactor is 335.26 g with a radius of 5 mm. Displacement history of the impactor is calculated by digital image correlation (DIC) with a commercial software VIC-2D (Correlated Solution Inc.) The impact velocity and impact force can be calculated from the first derivative and second derivative of displacement of the impactor, respectively.

### 2.4. Finite element analysis

The numerical simulations related to the mechanical response of the lattice reinforced composites under indentation tests are conducted using the commercial finite element (FE) package ABAQUS/Standard (Simulia, Providence, RI). Models with 20 × 10 unit cells with the same size of experimental specimens are used in all the simulations. All models are generated by plane strain elements CPE3H and meshed after a convergence test. In addition, geometric and material nonlinearities are taken into consideration to enable the precise simulation at large deformation of the structure. The constituent phases are taken to be a glassy polymer as the stiff phase and an elastomer material as the soft matrix. For each constituent material, isotropic material models are adopted. The stress-strain behavior of the glassy polymer is captured using an elastic-viscoplastic model which is exported from the true stress-strain relation of VeroWhite. The elastomeric stress-strain

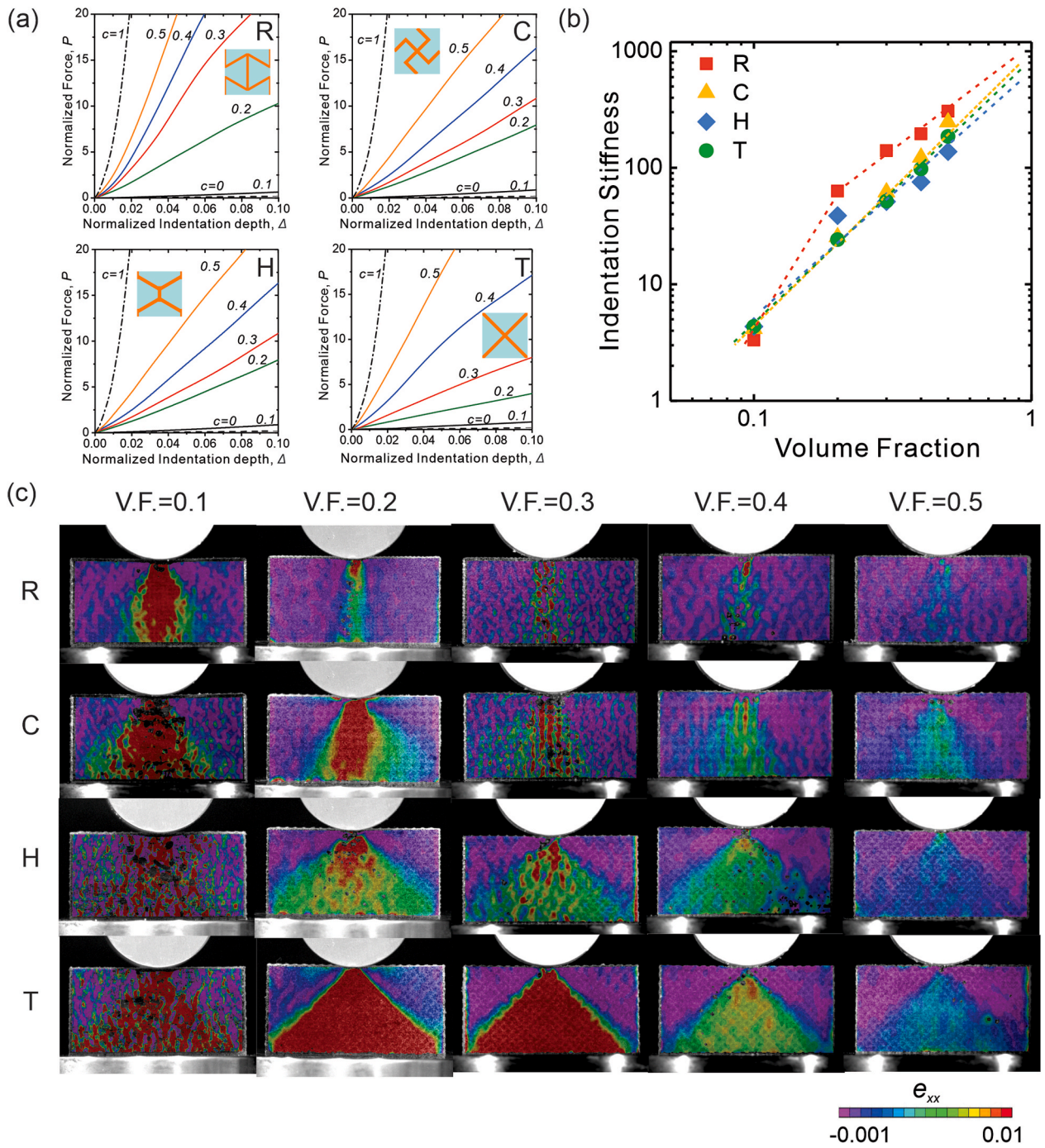


**Fig. 3.** Mechanical response of four types of composites at different volume fractions of the reinforcing phase during indentation tests. (a) Force *vs.* indentation depth for four different composites with re-entrant honeycomb, chiral truss, regular honeycomb, and regular truss designs. The curves are for composites with V.F. = 0.0, 0.1, 0.2, 0.3, 0.4, 0.5 and 1.0, respectively. (b) Relative indentation stiffness *vs.* volume fraction and composites with different lattice topology reinforcements. (c) Experimental strain contours (strain in the X-direction) of composites using digital image correlation at indentation depth, $\Delta = 0.05$. The images are composites with re-entrant honeycomb (R), chiral truss (c), regular honeycomb (H) and regular truss (T) designs in rows (1) to (4) – from top to bottom, respectively. The volume fraction, V.F. = 0.1, 0.2, 0.3, 0.4, 0.5 in column (1) to (5), from left to right, respectively.

behavior of TangoPlus is modeled as a hyperelastic material based on the Arruda-Boyce hyperelastic model [35] with an initial shear modulus of 0.213 MPa and locking stretch of 1.90. The cylindrical indenter is essentially modeled to be rigid. The surface-to-surface contact between the indenter surface and the specimens' upper surface is specified to be frictionless with no overclosure. To simulate the experimental conditions in the numerical analysis, a uniaxial displacement loading of the indenter is applied, while the bottom of the specimens is fixed along the vertical direction.

## 3. Results and discussion

### 3.1. Mechanical response of auxetic lattice reinforced composites

We first examine the indentation behavior of the lattice reinforced composites with re-entrant honeycomb, chiral lattice, regular honeycomb, truss lattice topology from an experimental standpoint (Fig. 2). Here, the same volume fraction of reinforcement phase of 20% is used for each composite design. In Fig. 2a, normalized force $P = F/(\mu t H)$ as a

function of normalized indentation depth, $\Delta = \delta/H$, is plotted, where the load, the shear modulus of the soft matrix and the displacement of the indenter are denoted by $F$, $\mu$ and $\delta$, respectively. Data are shown for three nominally identical specimens for each topology design, with the solid line corresponding to the mean response and the shaded region representing the scatter in data. The response of homogeneous cases with only constituent material TangoPlus (A) or VeroWhite (B) are also shown, which provides the lower limit and upper limit of indentation behavior, respectively. The specific lattice topology has a significant impact on the overall mechanical response of the lattice reinforced composites under indentation. The re-entrant honeycomb reinforced composites demonstrate clear superior over the other three composites, while the truss reinforced composite is more compliant. At large indentation depth, we notice load-drops for some structures. This is because the collapse of whole material in out-of-plane direction under compress of indenter. However, we focus on the indentation resistance of the material which is related to the material behavior under relatively small indentation depth. The dependence of the material resistance against indentation is further shown by plotting the relative indentation stiffness which is defined here as the secant stiffness, $C^{(P)}(\Delta) = \frac{P(\Delta)}{\Delta}$, and the relative indentation stiffness is given as the value relative to the indentation stiffness of the homogeneous case with pure material TangoPlus (A). Since the indentation stiffness changes with indentation depth, the indentation stiffness is considered at $\Delta = 0.01$. Fig. 2b quantitatively shows that the indentation stiffness of the re-entrant honeycomb reinforced composites is 1.4 times that of regular honeycomb reinforced composites, and 2.5 times those of chiral truss and regular truss reinforced composites, Moreover, the indentation stiffness of the chiral truss reinforced composites is slightly larger than that of regular truss reinforced composites. Because the re-entrant honeycomb lattice and the chiral truss lattice are two typical auxetic structures with negative Poisson's ratios, these results clearly show the advantage of employing auxetic lattice geometries especially re-entrant honeycomb structures in enhancing the indentation resistance of lattice reinforced composites.

Fig. 2c shows a series of images that exhibit the deformation behavior of these four lattice reinforced composites at indentation depth of 0.0, 0.05 and 0.4. Clearly the overall deformation behavior of these lattice reinforced composites at large deformation indentation is significantly different. At the same indentation depth, $\Delta = 0.4$, the re-entrant honeycomb reinforced composite exhibits no expansion of material in bottom side. The chiral truss reinforced composite has the asymmetry microstructures which shows a rotational deformation mechanism with a small bottom expansion in the left side. However, the regular honeycomb and the regular truss reinforced composites exhibit clearly large bottom expansion. These phenomena indicate that the auxetic lattice reinforced composites exhibit better indentation resistance compared with the non-auxetic lattice reinforced composites. Moreover, we have not observed any interfacial cracking between lattice and soft matrix on these multi-material composites in all the tests. The ink-jet multi-material printing process generates a graded transition area of mixing of both materials, which provides a perfect bonding between hard and soft materials. To further understand the indentation behavior of these lattice reinforced composites and capture the deformation in the microstructure, we use DIC to analyze the experimental strain contours for each composite under the indentation depth $\Delta = 0.05$. The auxetic reinforced composites (re-entrant honeycomb and chiral truss) show smaller strain in the lateral direction ($e_{xx}$), larger shear strain ($e_{xy}$) and smaller strain in the loading direction ($e_{yy}$) compared with the non-auxetic reinforced composites (regular honeycomb and truss). Moreover, in non-auxetic reinforced composites, large lateral expansion causes the flow of material away from the indent location which was observed in the specimens at large indentation depth. Therefore, these experimental strain contours indicate that the auxetic reinforced composites have less lateral expansion of microstructures under indentation loading which provides the better indentation resistance compared with the non-auxetic reinforced composites.

**Table 1**
Coefficients for the relations of the indentation stiffness to the volume fraction of the reinforcement phase ($\overline{\rho}$) for the lattice reinforced composites.

| | Re-entrant Honeycomb $0 \ll \overline{\rho} 0.2$ | $0.2 \ll \overline{\rho} 1$ | Regular Honeycomb $0 \ll \overline{\rho} 1$ | Chiral Truss $0 \ll \overline{\rho} 1$ | Regular Truss $0 \ll \overline{\rho} 1$ |
|---|---|---|---|---|---|
| $A$ | 10.981 | 6.604 | 6.447 | 6.791 | 6.6105 |
| $b$ | 4.248 | 1.453 | 2.060 | 2.251 | 2.193 |

### 3.2. Effect of volume fraction

It has been demonstrated that the auxetic lattice reinforced composites exhibit enhanced indentation resistance compared with non-auxetic lattice reinforced composites. While these results reported in Fig. 2 are for composites with the volume fraction of the reinforcement phase as 20%, further tunability can be achieved by altering the volume fraction of the reinforcement phase. Fig. 3 presents the responses to indentation for composites with re-entrant honeycomb (R), chiral truss (c), regular honeycomb (H) and regular truss (T) designs; and with V.F. = 0.0, 0.1, 0.2, 0.3, 0.4, 0.5 and 1.0, respectively. From the normalized force and normalized indentation depth relations as shown in Fig. 3a, it is clearly shown that the indentation force increases with an increase in volume fraction of lattice phase for each composite. The homogeneous case provides the lower limit of V.F. = 0.0, while the stiffest response is observed for the material with V.F. = 1.0. The relative indentation stiffness, $C$ are plotted with the volume fraction of the reinforcement phase, $\overline{\rho}$ in Fig. 3b. The re-entrant honeycomb reinforced composite shows the largest indentation stiffness in composites with V.F. $\geq$ 0.2 while the smallest indentation stiffness in composites with V.F. = 0.1 comparing to the other three composites. The chiral lattice reinforced composite is the second-best performing composites in general for indentation behavior. The non-auxetic lattice reinforced composites exhibit relative weak indentation stiffness comparing to their corresponding auxetic lattice reinforced composites. Generally, the Young's modulus of the cellular materials, such as metal foams and lattice structures, can be described by a scaling law between the mechanical property and the relative density [36]. Since the mechanical property of lattice reinforced composites is dominated by the reinforcement phase, we can use a scaling law to describe the response of these composites in this study. For the relative indentation stiffness, $C$ of the composite can be described as a function of the volume fraction of the reinforcement phase, $\overline{\rho}$, via $C = A\overline{\rho}^b$ where $A$ and $b$ can be obtained by fitting the experimental data, which are listed in Table 1. The scaling exponent $b$ close to 1 indicates a stretching dominated deformation behavior whereas an exponent of 2 typically indicates bending dominated deformation. It is also established that structures governed by a stretching dominated deformation offer higher mechanical properties per unit weight than those governed by bending dominated deformation. In our lattice reinforced composites, the scaling exponent, $b$ for re-entrant honeycomb reinforced composites are found to be 1.453 at $0.2 < \overline{\rho} < 1$ and 4.248 at $0 < \overline{\rho} < 0.2$. These results indicate that the re-entrant honeycomb reinforced composites are close to stretch-dominated deformation at large volume fraction of lattice phase. This is because the matrix phase is under biaxial compression which provides additional resistance of indentation and suppresses the bending and rotation of the ligaments of the lattice structures, making them more difficult to deform, switching the deformation mechanism to stretching dominated. However, when the volume fraction of lattice phase is smaller than 0.2, the stretching-dominated effect is weakened because the deformation is not completely dominated by the lattice reinforcement. While for the other composites, the scaling exponents are larger or

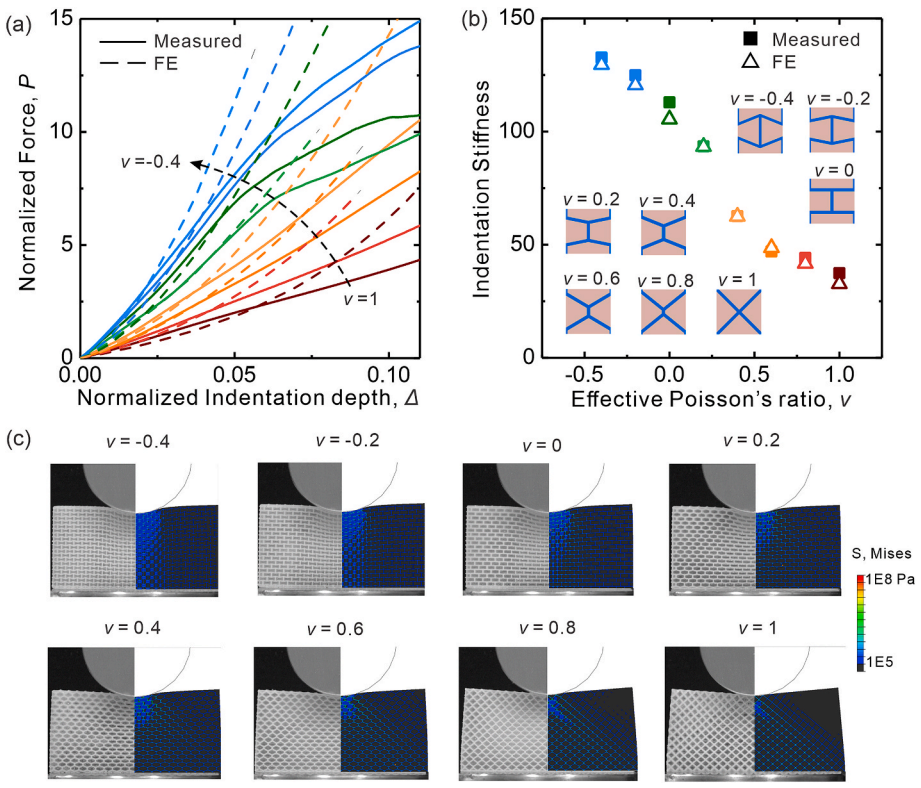


**Fig. 4.** Effect of Poisson's ratio on the mechanical properties of various honeycomb reinforced composites during indentation tests. (a) Comparison of the predicted and measured force *vs.* indentation depth for honeycomb reinforced composites with Poisson's ratio varying from −0.4 to 1. (b) Comparison of the predicted and measured relative indentation stiffness *vs.* effective Poisson's ratio. (c) Experimental deformation images and simulated von Mises stress contours for various honeycomb reinforced composites at indentation depth, $\Delta = 0.05$.

close to 2 at $0 \ll \bar{\rho} 1$. These results indicate that the deformation mechanism for these composites are close to bending-dominated under the indentation. In Fig. 3c, the strain contours in lateral direction for each composite design with certain volume fraction of lattice reinforcement are provided. Note that for each composite with increasing volume fraction of lattice reinforcement, the lateral strain decreases which indicate an enhanced indentation resistance. At the same volume fraction of lattice reinforcement, less lateral expansion of microstructures in auxetic reinforced composites promotes better indentation resistance compared with the non-auxetic reinforced composites. As a result, the deformation mechanism significantly affects the indentation response of the lattice reinforced composites. These results also suggest great potentials to tailor the volume fraction of lattice designs to achieve enhanced and tunable mechanical properties under indentation.

### 3.3. Effect of negative Poisson's ratio

It has been shown that the auxetic lattice reinforced composites exhibit enhanced indentation resistance with various volume fraction of lattice reinforcement compared with non-auxetic lattice reinforced composites. These improved mechanical properties are attributed to the rational structural design of the lattice reinforcement combined with the material selections for the reinforcements and matrix phases. In particular, the negative Poisson's ratio in the auxetic reinforcements is crucial to the unusual combination of mechanical performance. To quantitatively understand the effect of Poisson's ratio on the indentation behavior of the lattice reinforcement composites, we experimentally and numerically explore the response upon indentation tests of the composites reinforced by honeycombs with different Poisson's ratios achieved by varying lattice structure designs. Here we fix the same unit cell size and assume the value of Poisson's ratio of each cellular structure to achieve the exact lattice geometries based on Gibson's model [36]. Fig. 4 shows the corresponding design of honeycomb reinforced composite with Poisson's ratio from −0.4 to 1. The volume fraction of honeycomb reinforcement phase is 20% for each design for a fair comparison. The results reported in Fig. 4a exhibit the comparison of the predicted and measured normalized force and normalized indentation depth relations. Firstly, we notice the honeycomb lattice reinforced composites with smaller Poisson's ratio design exhibit better indentation performances. Second, the force-depth response between simulation and experiment agrees very well at the beginning in elastic deformation area. However, the simulation results show higher force response in large indentation depth than experimental results because in the simulation, we assume the plane strain condition. But in experimental tests, the thickness of the specimens is 15 mm actually. And at larger indentation depth, the out-of-plane deformation in experiment reduces the lateral compression and leads to the lower force-depth response. From the force-depth responses of all the designed composites, we have obtained the relations of indentation stiffness versus the Poisson's ratio of each composite design, as shown in Fig. 4b. Again, we noticed a very good agreement between the simulation and experiment. The relation also indicates that the honeycomb lattice composites with lower Poisson's ratios have improved indentation stiffness. For example, the indentation stiffness of the composite with a Poisson's ratio of −0.4 is 3 times of that of the composite with a Poisson's ratio of 1. Fig. 4c exhibits the deformation images of composites at indentation depth, $\Delta = 0.05$ from experiments and simulations. It is noticed the deformed shape of the composites with lower Poisson's ratio show less lateral expansion. From the von Mises stress contours, we can clearly see the composites with lower Poisson's ratio have larger stress concentration which is consist with the measured enhanced stiffness. These results offer a complete picture of the effect of Poisson's ratio on the indentation response of the lattice reinforced composites.

### 3.4. Dynamic indentation behavior of auxetic lattice reinforced composites

To understand the mechanical performance of these composites under dynamic indentation/impact tests, the dynamic indentation results of these composites with a series of impact velocity, $v_{input} = 3, 5, 8,$

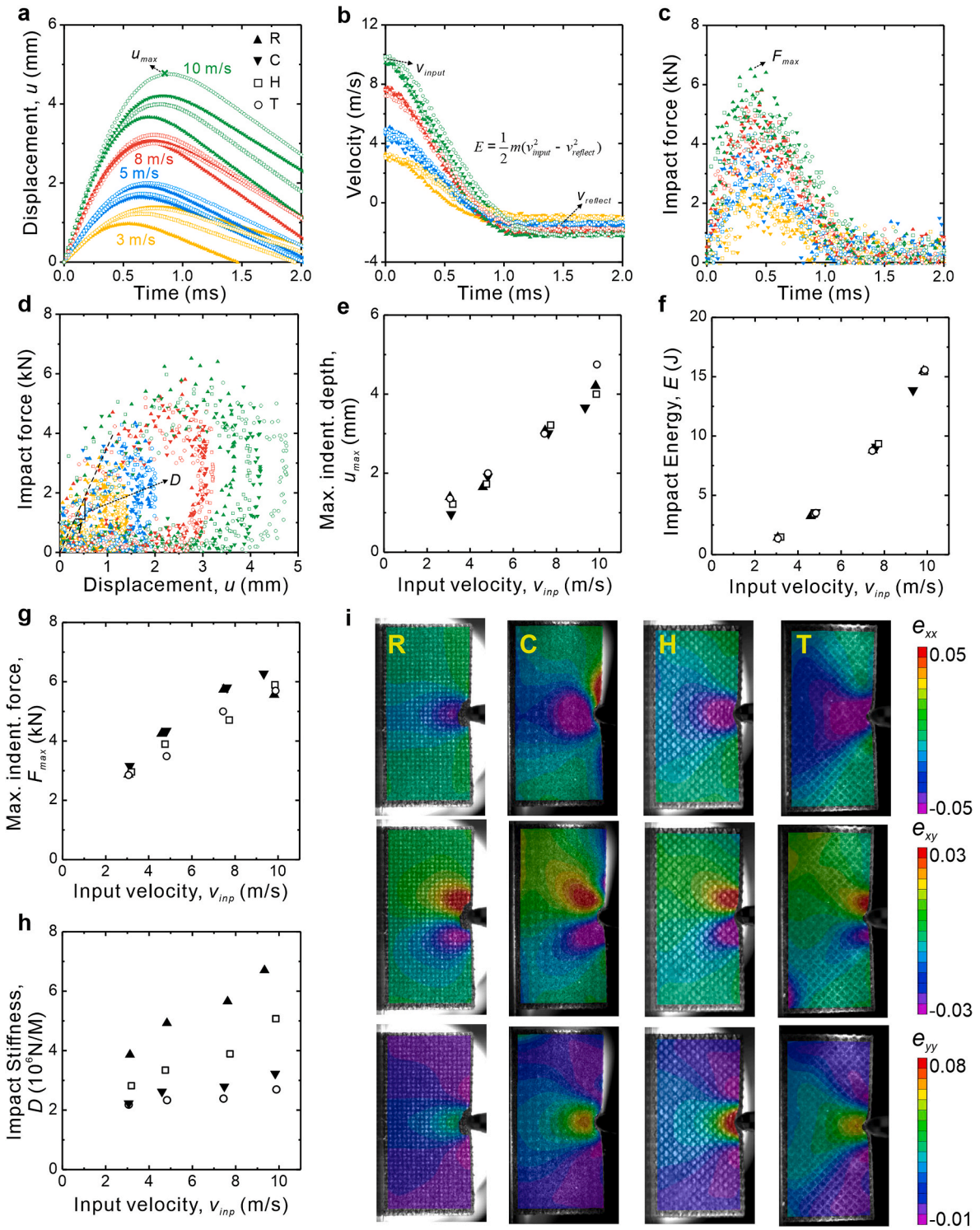


**Fig. 5.** Mechanical response of the 3D-printed lattice reinforced composites under dynamic indentation tests with an indenter of $m = 335$ g at different impact velocity, $v_{input} = 3, 5, 8, 10$ m/s. For four different composites with re-entrant honeycomb, chiral truss, regular honeycomb, regular truss designs, (a) displacement history, (b) velocity history, and (c) impact force history are measured from the tests. Calculated from the three histories, (d) impact force *vs.* displacement; (e) max. indentation depth *vs.* impact velocity; (f) impact energy *vs.* impact velocity; (g) max. indentation force *vs.* impact velocity and (h) relative impact stiffness *vs.* impact velocity are plotted. (i) Experimental strain contours of composites at $v_{input} = 3$ m/s using digital image correlation at indentation depth, $\Delta = 0.05$.

10 m/s are summarized in Fig. 5. From the recorded videos, the displacement, velocity and force histories of the indenter can be calculated, which are further used to characterize the dynamic parameters (Fig. 5a–c). Dynamic performances (Fig. 5d–h) are evaluated from histories relations. For examples, the maximum indentation displacement is achieved from the peak point of displacement histories. The absorbed impact energy is estimated as the kinetic energy loss, $E_{ab} = \frac{1}{2}mv_{input}^2 - \frac{1}{2}mv_{reflect}^2$, where $v_{input}$ and $v_{reflect}$ are the initial and reflect velocity of the impactor and $m$ is the mass of the impactor. The maximum indentation force is evaluated from the peak force of the force histories relations. The impact stiffness is calculated as the slope of the initial linear parts of

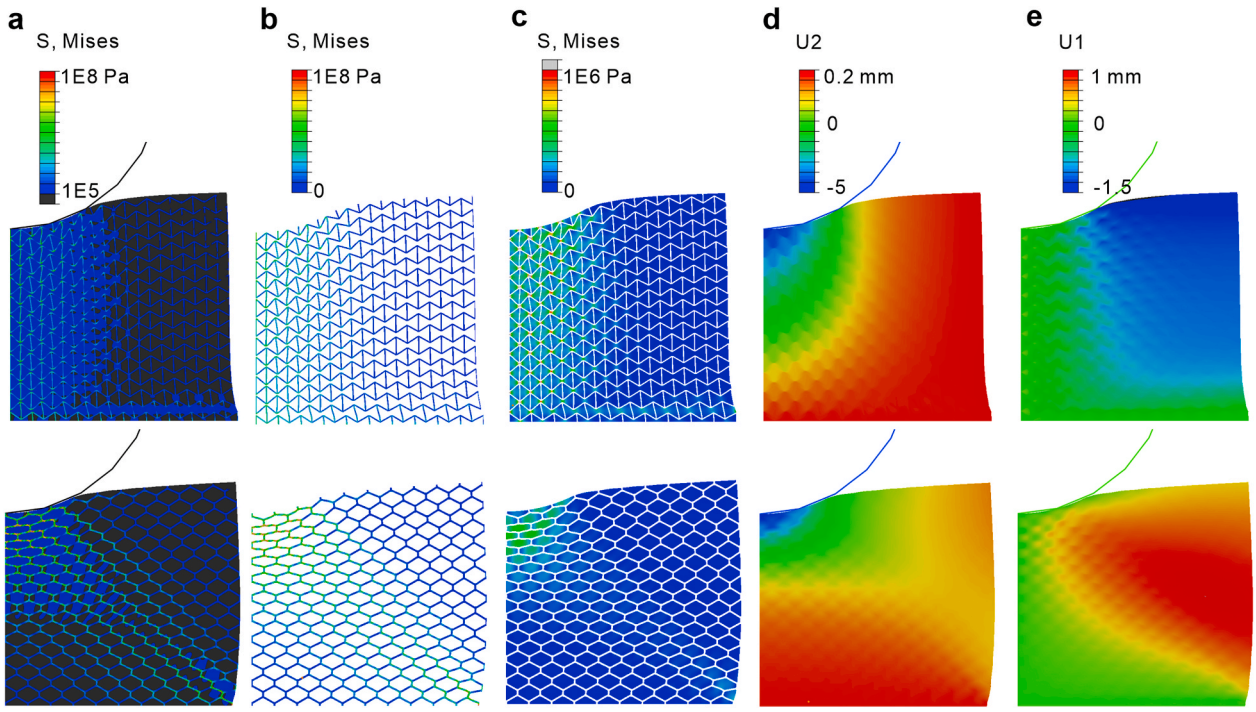


**Fig. 6.** Numerical results of re-entrant honeycomb and regular honeycomb reinforced composites under indentation depth, $\Delta = 0.15$. Comparison of the von Mises stress distribution for (a) composites, (b) reinforcement phases and (c) matrix phases. Comparison of displacement contours for (d) the direction of indent and (e) the direction perpendicular to the indent.

force versus displacement relations. It is clearly noticed that the auxetic lattice reinforced composites exhibit smaller maximum indentation displacement, larger maximum indentation force compared with their non-auxetic counterparts. The absorbed impact energy for all the specimens are around the same at each impact velocity. The impact stiffness for auxetic lattice reinforced composites are higher than their non-auxetic counterparts at each impact velocity. While the impact stiffness of these composites increases when the input velocity of indenter increases which indicates that these 3D printed materials are highly strain-rate dependent. The experimental strain contours (Fig. 5i) are very similar to the results in the static indentation tests (Fig. 2c). The auxetic reinforced composites (re-entrant honeycomb and chiral truss) show smaller strain in the lateral direction ($e_{xx}$), larger shear strain ($e_{xy}$) and smaller strain in the loading direction ($e_{yy}$) compared with their non-auxetic counterparts (regular honeycomb and truss), respectively. These results suggest good ability to employ auxetic lattice reinforced composites to achieve enhanced dynamic indentation performances for purposeful mechanical applications.

### 3.5. *Mechanism for enhanced indentation performance of auxetic lattice reinforced composites*

To explain these enhanced performances, numerical simulations are performed on these auxetic and non-auxetic honeycomb reinforced composites under indentation. Fig. 6 shows that these improved indentaion performance is attributed to two underlying mechanisms. On one hand, the negative Poisson's ratio effect of the auxetic reinforcements, which makes the matrix in a state of biaxial compression and hence provides additional support. It is clearly noticed from the Mises stress contour, the matrix phase of the auxetic composites has higher stress concentration in larger volume of material than that of the non-auxetic composites, as seen in Fig. 6c. On another hand, the overall negative Poisson's effect of the auxetic composites makes the material 'flows' into the vicinity of the indent. It can be clear seen that the lateral displacement (U1) is negative/positive for auxetic composites/non-auxetic composites, respectively as seen in Fig. 6e. In auxetic materials, these material gathering creates an area of denser material and produces the higher stress concentration in larger areas (Fig. 6a and b) which is resistant to indentation. Finally, our simulation can uncover the underlying mechanism of the indentation enhancement of auxetic lattice reinforced composites observed from the experiments.

Furthermore, we need to emphasize three significant factors: the material stiffness ratio, the incompressible rubber-like matrix and the bonding behavior between lattice and matrix strongly determine whether the mechanical enhancement of auxetic composite over non-auxetic counterparts exist. First, in one recent numerical study [37] about the effect of stiffness ratios on the overall mechanical properties of re-entrant honeycomb composites, it is found when the stiffness ratio is smaller than 1000, the auxetic effect disappears; while the normalized effective Young's modulus and shear modulus of composite decreases with increasing the stiffness ratio. Clearly in our case, the stiffness ratio is around 2000 (modulus of VeroWhite over modulus of TangoPlus) which provides the composite with auxetic behavior and enhanced modulus. Both auxetic effect and certain modulus are important to create a composite with enhanced indentation stiffness. Secondly, in our study the matrix, TangoPlus, is a type of incompressible rubber-like polymer. This incompressible infill implies a fixed infill volume and a change in deformation mode. For example, the deformation for re-entrant honeycomb composite is stretching dominated comparing with bending and hinge rotation dominated deformation in re-entrant honeycomb lattice. Consequently, a change in mode gives the composite synergistic strengthening which is not only simple mixture of lattice and matrix materials. Thirdly, the perfect material bonding in our multi-material 3D printed composites enables better mechanical performance compared with conventional infilled lattice-matrix composites in which interface failure is critical. For example, the mechanical properties of epoxy infilled metal auxetic lattice exhibit only slightly increased energy absorption ability during impact tests [38] because of less bonding forces between common epoxy and metal, which makes the composite lose the additional support from the matrix after interfacial cracking. Therefore, the mechanical enhancement of auxetic lattice reinforced composite is strongly depending on both the material

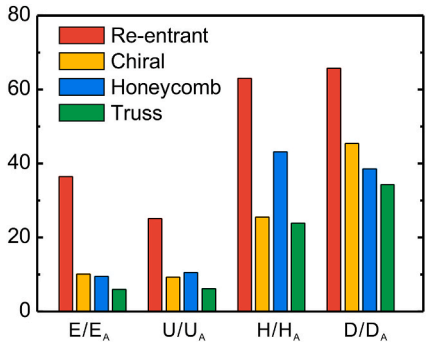


**Fig. 7.** Mechanical properties for the four type of lattice reinforced composites including re-entrant honeycomb, chiral, regular honeycomb and truss lattices: stiffness *E*, energy absorption *U*, indentation stiffness/hardness *H* and impact stiffness *D* at the impact velocity of 3 m/s. The data is normalized by the respective values for the base material A (matrix phase).

selection and the manufacturing method for the lattice and matrix phases.

## 4. Conclusions

Auxetic materials have drawn a lot of research interest, however, they usually exhibit lower stiffness comparing with their non-auxetic counterparts, limiting their applications in structural engineering. We have designed and additive manufactured a series 3D printed multi-material composites which consist lattice structures as reinforcements and soft matrix. We find that the auxetic lattice structures including re-entrant honeycomb and chiral truss exhibit better mechanical performance compared with the non-auxetic lattice structures including regular honeycomb and regular truss. In details from Fig. 7, we show a bar plot comparing select mechanical characteristics from the experimentally compression [2] and indentation tests for four lattice reinforced composites respectively. The re-entrant honeycomb reinforced composites exhibit the highest stiffness, energy absorption, static and dynamic indentation stiffness compared with the other three composites. Moreover, the chiral truss reinforced composites also exhibit better mechanical performance compared with the regular truss reinforced composites.

Furthermore, we use scaling law to evaluate the effect of volume fraction of the reinforcement phase on the indentation stiffness of the composites, showing that the re-entrant honeycomb reinforced composite exhibit nearly linear scaling at large volume fraction of stiff phase ($>0.2$). We also quantify the effect of Poisson's ratio on the indentation behavior of various honeycomb reinforced composites, indicating that the negative Poisson's ratio of the composites would result in enhanced indentation stiffness.

Finally, we discover the underlying mechanisms for excellent mechanical performance of auxetic lattice reinforced composites by performing digital image processing of experimental tests and the corresponding numerical simulations. On one hand, the negative Poisson's ratio effect of the auxetic reinforcements makes the matrix in a state of biaxial compression during indentation/impact and hence provides additional support. On another hand, the negative Poisson's ratio effect of the overall composites makes the auxetic reinforced composites denser at the site of the indentation/impact and therefore more resistant to indentation.

Therefore, we conclude that the design strategy of using auxetic lattice structures as reinforcement is an effective way to develop novel composites with enhanced mechanical performance for a wide range of mechanical and structural applications.

## Author statement

**Tiantian Li**: Conceptualization, Methodology, Investigation, Formal analysis, Visualization, Writing - Original Draft.

**Fan Liu**: Methodology, Investigation, Formal analysis.

**Lifeng Wang**: Conceptualization, Methodology, Investigation, Supervision, Validation, Writing - review & editing.

## Declaration of competing interest

The authors declare that they have no known competing financial interests or personal relationships that could have appeared to influence the work reported in this paper.

## Acknowledgements

This research was partly supported by the National Science Foundation (CMMI-1437449, CMMI-1462270). The authors acknowledge the use of the Center for Functional Nanomaterials facility at Brookhaven National Laboratory. T. Li thanks Dr. Zian Jia and Dr. Shaoyu Hou for their assistance in setting up the SHPB apparatus and impact tests.

## Appendix A. Supplementary data

Supplementary data related to this article can be found at https://doi.org/10.1016/j.compositesb.2020.108229.

## References

[1] Kuribayashi K, Tsuchiya K, You Z, Tomus D, Umemoto M, Ito T, et al. Self-deployable origami stent grafts as a biomedical application of Ni-rich TiNi shape memory alloy foil. Mater Sci Eng, A 2006;419(1):131–7.
[2] Li T, Chen Y, Hu X, Li Y, Wang L. Exploiting negative Poisson's ratio to design 3D-printed composites with enhanced mechanical properties. Mater Des 2018;142:247–58.
[3] Evans KE, Nkansah MA, Hutchinson IJ. Auxetic foams: modelling negative Poisson's ratios. Acta Metall Mater 1994;42(4):1289–94.
[4] Sanami M, Ravirala N, Alderson K, Alderson A. Auxetic materials for sports applications. Procedia Eng 2014;72:453–8.
[5] Jiang Y, Liu Z, Matsuhisa N, Qi D, Leow WR, Yang H, et al. Auxetic mechanical metamaterials to enhance sensitivity of stretchable strain sensors. Adv Mater 2018;30(12):1706589.
[6] Zhang SL, Lai Y-C, He X, Liu R, Zi Y, Wang ZL. Auxetic foam-based contact-mode triboelectric nanogenerator with highly sensitive self-powered strain sensing capabilities to monitor human body movement. Adv Funct Mater 2017;27(25):1606695.
[7] Ugbolue SC, Kim YK, Warner SB, Fan Q, Yang C-L, Kyzymchuk O, et al. The formation and performance of auxetic textiles. Part I: theoretical and technical considerations. J Textil Inst 2010;101(7):660–7.
[8] Baughman RH, Shacklette JM, Zakhidov AA, Stafström S. Negative Poisson's ratios as a common feature of cubic metals. Nature 1998;392(6674):362–5.
[9] Grima JN, Jackson R, Alderson A, Evans KE. Do zeolites have negative Poisson's ratios? Adv Mater 2000;12(24):1912–8.
[10] Song F, Zhou J, Xu X, Xu Y, Bai Y. Effect of a negative Poisson ratio in the tension of ceramics. Phys Rev Lett 2008;100(24):245502.
[11] Yeganeh-Haeri A, Weidner DJ, Parise JB. Elasticity of α-cristobalite: a silicon dioxide with a negative Poisson's ratio. Science 1992;257(5070):650–2.
[12] Grima JN, Winczewski S, Mizzi L, Grech MC, Cauchi R, Gatt R, et al. Tailoring graphene to achieve negative Poisson's ratio properties. Adv Mater 2015;27(8):1455–9.
[13] Suzuki Y, Cardone G, Restrepo D, Zavattieri PD, Baker TS, Tezcan FA. Self-assembly of coherently dynamic, auxetic, two-dimensional protein crystals. Nature 2016;533(7603):369–73.
[14] Lakes R. Foam structures with a negative Poisson's ratio. Science 1987;235:1038–41.
[15] Chan N, Evans KE. Fabrication methods for auxetic foams. J Mater Sci 1997;32(22):5945–53.
[16] Gibson LJ, Ashby MF, Schajer GS, Robertson CI. The mechanics of two-dimensional cellular materials. Proc Roy Soc Lond Math Phys Sci 1982;382(1782):25–42.
[17] Prall D, Lakes RS. Properties of a chiral honeycomb with a Poisson's ratio of — 1. Int J Mech Sci 1997;39(3):305–14.
[18] Chen Y, Li T, Scarpa F, Wang L. Lattice metamaterials with mechanically tunable Poisson's ratio for vibration control. Phys Rev Appl 2017;7(2):024012.
[19] Li T, Hu X, Chen Y, Wang L. Harnessing out-of-plane deformation to design 3D architected lattice metamaterials with tunable Poisson's ratio. Sci Rep 2017;7(1):8949.

[20] Grima JN, Alderson A, Evans KE. Auxetic behaviour from rotating rigid units. Phys Status Solidi 2005;242(3):561–75.
[21] Yasuda H, Yang J. Reentrant origami-based metamaterials with negative Poisson's ratio and bistability. Phys Rev Lett 2015;114(18):185502.
[22] Cho Y, Shin J-H, Costa A, Kim TA, Kunin V, Li J, et al. Engineering the shape and structure of materials by fractal cut. Proc Natl Acad Sci Unit States Am 2014;111(49):17390–5.
[23] Wang YC, Lakes RS. Composites with inclusions of negative bulk modulus: extreme damping and negative Poisson's ratio. J Compos Mater 2005;39(18):1645–57.
[24] Choi JB, Lakes RS. Fracture toughness of re-entrant foam materials with a negative Poisson's ratio: experiment and analysis. Int J Fract 1996;80(1):73–83.
[25] Alderson A, Alderson KL, Chirima G, Ravirala N, Zied KM. The in-plane linear elastic constants and out-of-plane bending of 3-coordinated ligament and cylinder-ligament honeycombs. Compos Sci Technol 2010;70(7):1034–41.
[26] Alderson A, Rasburn J, Evans KE, Grima JN. Auxetic polymeric filters display enhanced de-fouling and pressure compensation properties. Membr Technol 2001;2001(137):6–8.
[27] Li T, Wang L. Bending behavior of sandwich composite structures with tunable 3D-printed core materials. Compos Struct 2017;175:46–57.
[28] Hou S, Li T, Jia Z, Wang L. Mechanical properties of sandwich composites with 3d-printed auxetic and non-auxetic lattice cores under low velocity impact. Mater Des 2018;160:1305–21.
[29] Alderson A. A triumph of lateral thought. Chem Ind 1999:384–91.
[30] Evans KE, Alderson A. Auxetic materials: functional materials and structures from lateral thinking! Adv Mater 2000;12(9):617–28.
[31] Alderson KL, Pickles AP, Neale PJ, Evans KE. Auxetic polyethylene: the effect of a negative Poisson's ratio on hardness. Acta Metall Mater 1994;42(7):2261–6.
[32] Chan N, Evans KE. Indentation resilience of conventional and auxetic foams. J Cell Plast 1998;34(3):231–60.
[33] Lakes RS, Elms K. Indentability of conventional and negative Poisson's ratio foams. J Compos Mater 1993;27(12):1193–202.
[34] Jia Z, Li T, Chiang F-p, Wang L. An experimental investigation of the temperature effect on the mechanics of carbon fiber reinforced polymer composites. Compos Sci Technol 2018;154:53–63.
[35] Wang L, Lau J, Thomas EL, Boyce MC. Co-continuous composite materials for stiffness, strength, and energy dissipation. Adv Mater 2011;23(13):1524–9.
[36] Gibson LJ, Ashby MF. Cellular solids: structure and properties. Cambridge University Press; 1999.
[37] Peng X-L, Soyarslan C, Bargmann S. Phase contrast mediated switch of auxetic mechanism in composites of infilled re-entrant honeycomb microstructures. Extreme Mech Lett 2020;35:100641.
[38] Fíla T, Zlámal P, Jiroušek O, Falta J, Koudelka P, Kytýř D, et al. Impact testing of polymer-filled auxetics using split Hopkinson pressure Bar. Adv Eng Mater 2017;19(10):1700076.